**Proceedings of the ASME 2018 International Design Engineering Technical Conferences and Computers and Information in Engineering Conference**
**IDETC/CIE 2018**
**August 26-29, 2018, Quebec City, Quebec, Canada**

**DETC2018-85568**

# OPTIMAL NON-UNIFORM PARAMETRIZATION FOR FOURIER DESCRIPTOR BASED PATH SYNTHESIS OF FOUR BAR MECHANISMS

**Shashank Sharma, Anurag Purwar*, Q. Jeffrey Ge**
Computer-Aided Design and Innovation Lab
Department of Mechanical Engineering
Stony Brook University
Stony Brook, New York, 11794-2300

## ABSTRACT

*Fourier descriptor based path synthesis algorithms rely on harmonic decomposition of four-bar loop closure equation to split the design space into smaller subsets. The core of the methodology depends on calculation and fitting of Fourier descriptors. However, a uniform time parametrization is assumed in existing literature. This paper aims to explore the use of non-uniform time parametrization of input data and calculation of an optimal parametrization. Additionally, design-centric constraints have been proposed to give user enhanced control over coupler speed. As a result, this work improves the existing algorithm tremendously.*

**Keywords**: Planar four-bar linkage, Open and Closed path generation, Non uniform Fourier descriptor, optimal parametrization.

## 1 Introduction

Mechanism synthesis problem can mostly be classified into path, motion and function synthesis problems. Each of these problems has been too complex to be solved for a generalized $n$-bar one-degree-of-freedom mechanism. Consequently, most of the work done deals with synthesis problem for the simplest case in the family of all one degree of freedom mechanisms, the four-bar mechanism. Different types of possible joints (revolute or prismatic) and coupler point motion (closed or open) introduces further complexities into the system. Many analytic and approximate approaches have been proposed in an attempt to solve these problems. In this paper, the focus is on path synthesis problems for four-bar mechanisms for open and closed paths. Linkages involving only revolute joints are considered.

Analytical methods for synthesis include algebraic methods [1,2,3], complex number methods [4] or displacement matrix methods [5]. However, they can handle only up to 9 path points above which the system of equations becomes over-constrained. Even the exact results up to 9 path points are extremely complex and can rarely be calculated. To counter these drawbacks, path synthesis problem can be solved using an approximation. These methods can handle any number of path points. However, compromise on precision is made in favor of approximate solutions.

Most of the approximation techniques restructure the synthesis problem into an optimization problem [6, 7, 8, 9, 10, 11, 12, 13, 14, 15, 16]. These techniques are characterized by a variety of domain space variables, objective function and optimization algorithm. Domain space variables depend on the formulation of problem. Objective function is the measure of how good a prospective mechanism is in fulfilling the target path requirements using domain space variables. Optimization algorithm can be broadly classified as global/local or deterministic/stochastic. There is no best algorithm and use of each depends on problem. A fast, accurate and easy to code/formulate optimization is desirable.

In practical problems, the designer is interested in the general shape of coupler path rather than a small number of precision points on coupler path. Thus, path synthesis can be formulated

*Address all correspondence to this author.

 

as a problem in the area of Shape Analysis [13, 16, 17, 18, 19] by fitting a curve using path points. By converting point fitting problem to curve matching problem, possible output mechanisms are constrained to practical 'smooth' choices and usually rejects huge displacements in between precision points or defects. For comparison, a metric need to be established which approaches zero when two curves match. Various metrics like distance measures, Fourier descriptors [20], wavelets [21], cumulative angular deviant [13], etc. have been used over the years to compare two curves. Frechet distance, Dynamic time warping or Euclidean distance are the predominant distance measures which have been used for curve matching using point sampling [22].

This paper focuses on solving the path synthesis problem using Fourier based path approximation on which prominent work has been done by [23, 24, 25]. The Fourier based path synthesis algorithm is a two step process. First, an optimum task path using the user-input path points is calculated. The subsequent motivation is to find a mechanism whose coupler path closely approximates the task path. However, finding the task curve using Fourier transformation requires time parametrization.

Fourier based path synthesis implementations in previous publications assume a uniformly sampled data, i.e., the time parameters attached to the given points are assumed to be uniform. As a consequence, the Fourier curve carries over time information to the path. In a purely geometric sense, this behavior is undesired. Although the problem has been mentioned in [25] no work has been done to find a parametrization independent representation until very recently in [26], where an approach to eliminate time dependency has been proposed. They try to use arc length parametrization to capture the geometric features and eliminate the time parameter. However, it is well-known that the task curves cannot be arc-length parameterized analytically and converted into unit speed curves. Thus, the authors numerically *guess* the arc length parametrization using the task point polygon and thus fail to get a time-independent parametrization.

This paper makes original contribution in three areas: 1) the formulation of a generalized parametrization scheme for non-uniform Fourier decomposition based path synthesis algorithm and calculation of optimal task curve. 2) the use of proposed methodology to generate multiple solutions for same input path points. 3) the incorporation of design centric constraints in the mathematical framework for greater control over synthesized mechanism speed.

Rest of this paper is organized as follows. Section 2 reviews the existing Fourier based path synthesis algorithm. Section 3 introduces a family of parameterizations and establishes a metric to select the optimum among them. Section 4 proposes additional design-centric constraints to help control synthesized mechanism's speed over its path. Section 5 discusses examples and analyzes the fitting of target curve using uniform parametrization and the proposed optimal parametrization.

## 2 Fourier based Path Synthesis

In this section, a brief overview of existing Fourier based path synthesis algorithm is presented. For an in-depth discussion, refer to work done by [23, 24, 25].

### 2.1 Approximation of Task Path

The initial objective is to convert input points into a task path i.e. a curve representing user's intended path. Path points input by the user can vary from one to infinity. For one to three points, the solution curve is a circle and the mechanism is an RR dyad. Thus, mechanism synthesis of four or more input path points is of interest.

A Task curve described using Fourier bases can be fitted to these input points as follows

$$z\left(\frac{2\pi k}{N}\right) = \sum_{m=-\infty}^{\infty} a_m e^{mi\left(\frac{2\pi k}{N}\right)} \qquad \forall \quad k \in [0, N-1]. \tag{1}$$

Here, $z = x + iy$ denote the input path points in complex form where $x$ and $y$ are the coordinates. $m$ are the frequencies, $a_m$ are the Fourier coefficients, $k$ is the sample point index and $N$ is the total number of sample points. The $\|m\|^{th}$ frequency is called as Harmonics. For example, first harmonic involves the curves described by frequencies $m = 1, -1$. Thus, a series of points can easily be used to recover the curve they represent using Discrete Fourier Transform (DFT).

To find the Fourier coefficients attached to Fourier bases, inverse discrete Fourier transform can be calculated using

$$a_m = \frac{1}{N} \sum_{k=0}^{N-1} z_k e^{-mi\left(\frac{2\pi k}{N}\right)}. \tag{2}$$

To incorporate both open and closed paths, trigonometric polynomial curves with an open interval are used to describe the task curve as shown below

$$z(t) = \sum_{m=-p}^{p} \alpha_m e^{\omega_o mit} \qquad \forall \quad t \in [0, T], T < 1. \tag{3}$$

Here, $T$ is the interval over which the curve is defined. In practice, task curve is defined using finite number of Fourier basis which is denoted by $p$. Literature indicates that seven harmonics capture the four bar path very accurately and is deemed sufficient.

The coefficients $\alpha_m$ to trigonometric bases are referred to as Fourier descriptors of task curve. These descriptors are calculated using least square fitting approach which can be formulated as

$$\Delta = \sum_{i=1}^{n} \left\| z(t_i) - \sum_{k=-p}^{p} \alpha_k e^{ik\omega_o t_i} \right\|^2. \tag{4}$$

Analytically solving the least square problem gives a linear system of equation. This can be solved to find the descriptors which best fits the input path points. This system of equation can be defined as follows

$$\Omega \mathbb{X} = \mathbb{Y}, \tag{5}$$

where

$$\mathbb{X} = [\ldots, \underset{m\rightarrow}{\alpha_m}, \ldots]^T, \tag{6}$$

$$\Omega = \underset{k\rightarrow}{\begin{bmatrix} & \cdots & \\ \vdots & \sum_{i=0}^{n} e^{i(k-m)\theta_i} & \vdots \\ & \cdots & \end{bmatrix}} \downarrow m, \tag{7}$$

$$\mathbb{Y} = [\ldots, \underset{m\rightarrow}{\sum_{i=0}^{n} z(t_i) e^{-im\theta_i}}, \ldots]^T. \tag{8}$$

Here, $k$ and $m$ vary from $-p$ to $p$. LU decomposition can be used to solve the above system.

The domain for the open task path representing input path points remains unknown and can range anywhere from $(0, 2\pi]$. Finding this domain $(T)$ is a one-dimensional optimization problem for minimum error measure defined in Eq. (4). Once the parameter distribution and total domain of open curve are calculated, the target curve is fully defined.

### 2.2 Approximation of Coupler Path

In this section, equation of coupler point for a four-bar mechanism is approximated using its loop closure equation. The mechanism is represented by the design parameters $x_0$, $y_0$, $l_1$, $l_2$, $l_3$, $l_4$, $r$, $\theta_1$, $\alpha$, $\phi_0$ as displayed in Fig. 1.

The analytic equation of coupler point P can be given as

$$P = A_0 + l_2 e^{i\theta_1} e^{i\phi} + r e^{i\alpha} e^{i\theta_1} e^{i\lambda}, \tag{9}$$

$$A_0 = x_0 + iy_0, \tag{10}$$

$$\phi = \phi_0 + \omega t. \tag{11}$$

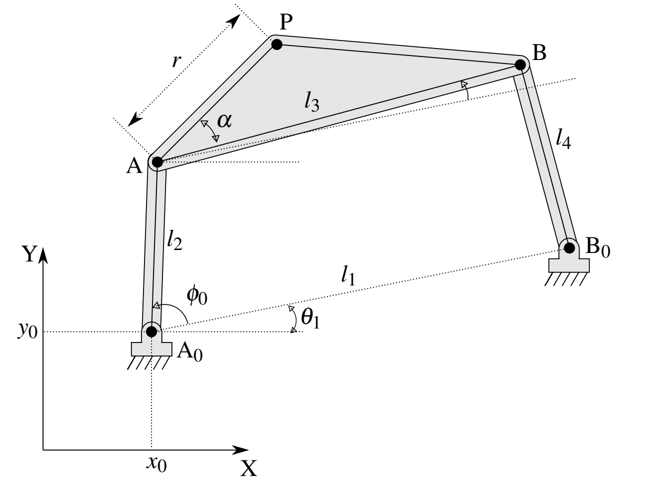


**FIGURE 1**: Visualization of parameters describing a four-bar mechanism

Finding the relation between coupler angle $(\lambda)$ and input crank angle $(\phi)$ leads to the expression

$$e^{i\lambda} = \frac{-B(\phi) \pm \sqrt{\Delta_1(\phi)\Delta_2(\phi)}}{2A(\phi)}, \tag{12}$$

where

$$A(\phi) = l_3(l_2 e^{-i\phi}) - l_1, \tag{13}$$

$$B(\phi) = l_1^2 + l_2^2 + l_3^2 - l_4^2 - 2l_1 l_2 \cos(\phi), \tag{14}$$

$$\Delta_1(\phi) = l_1^2 + l_2^2 - (l_3 + l_4)^2 - 2l_1 l_2 \cos(\phi), \tag{15}$$

$$\Delta_2(\phi) = l_1^2 + l_2^2 - (l_3 - l_4)^2 - 2l_1 l_2 \cos(\phi). \tag{16}$$

The $\pm$ sign in the equation represents the two different configurations of a four bar mechanism. It must be noted that this function is periodic as it consists of only trigonometric functions.

However, the Eq. (12) only gives meaningful results when the following feasibility condition is followed

$$\Delta_1(\phi)\Delta_2(\phi) \leq 0. \tag{17}$$

Thus, this Eq. (17) constraints the interval over which angle $\phi$ exist. The maximum it can range is $[0, 2\pi]$ in the case it represents a closed curve.

Eq. (12), being a periodic function when $\phi$=$[0, 2\pi]$, can be rewritten using Fourier basis as

$$e^{i\lambda} = \sum_{k=-\infty}^{\infty} C_k e^{ik\phi}. \tag{18}$$

Only a small group of $C_k$ associated with low harmonics is considered to approximate $e^{i\lambda}$, just like in approximation of task path. When $\phi$ varies only in some part of [0,$2\pi$], the least square curve fitting method is used to calculate coefficients. The coefficients $C_k$ are calculated numerically by sampling points on the function according to the previous parametrization, evaluating the function on each point based on crank angle and length ratios and then least square curve fitting the results to get an approximate solution. Finding an analytic closed form solution for each coefficient $C_k$ is not possible.

Using the Eqns. (12) and (18), we obtain

$$P = \sum_{k=-\infty}^{\infty} P_k e^{ik\omega t}, \tag{19}$$

where

$$P_0 = re^{i\alpha} e^{i\theta_1} C_0 + A_0, \tag{20}$$

$$P_1 = re^{i\alpha} e^{i\theta_1} C_1 e^{i\phi_0} + l_2 e^{i(\theta_1+\phi_0)}, \tag{21}$$

$$P_k = re^{i\alpha} e^{i\theta_1} C_k e^{ik\phi_0}|_{k\neq 0,1}. \tag{22}$$

Thus, an analytic expression has been obtained to describe the coupler curve using the mechanism parameters $x_0$, $y_0$, $l_1$, $l_2$, $l_3$, $l_4$, $r$, $\theta_1$, $\alpha$, $\phi_0$.

### 2.3 Fitting Coupler Path to Task path

The objective is to fit analytical coupler curve to the task curve. The Task curve $T$ and Coupler path $P$ have been calculated as

$$T \approx \sum_{k=-p}^{p} T_k e^{ik\Phi}, \tag{23}$$

$$P \approx \sum_{k=-p}^{p} P_k e^{ik\omega t}, \tag{24}$$

where $T_k$ are Task Curve descriptors and $P_k$ are Coupler Curve descriptors. $\Phi$ and $\omega t$ lies in range [0,$\Phi_{max}$] where $\Phi_{max}$ can lie anywhere between (0,$2\pi$].

Since $\phi = \phi_0 + \omega t$, range of $\phi$ i.e. input angle for mechanism is [$\phi_0$, $\phi_0 + \Phi_{max}$]. It should be noted that the exact value of input angle to reach each coupler point depends on the parametrization of samples i.e. $\Phi_i$.

For a perfect curve matching, $T_k = P_k$ for all $k \in [-p, p]$. This leads to

$$T_0 = C_0 re^{i\alpha} e^{i\theta_1} + A_0, \tag{25}$$

$$T_1 = C_1 re^{i\alpha} e^{i\theta_1} e^{i\phi_0} + l_2 e^{i(\theta_1+\phi_0)}, \tag{26}$$

$$T_k = C_k re^{i\alpha} e^{i\theta_1} e^{ik\phi_0}|_{k\neq 0,1}. \tag{27}$$

Following are the design parameters for a four-bar mechanism.

$$S = \left\{ l_2, \frac{l_2}{l_1}, \frac{l_3}{l_1}, \frac{l_4}{l_1}, x_0, y_0, \theta_1, \phi_0, r, \alpha \right\}. \tag{28}$$

However, we use a slightly modified form of the parameters in this paper as following:

$$S = \left\{ l_2, \frac{l_2}{l_1}, \frac{l_3}{l_1}, \frac{l_4}{l_1}, x_0, y_0, \theta_1, \phi_0, \mathbb{C}, \mathbb{S} \right\}, \tag{29}$$

where

$$\mathbb{C} = r\cos\alpha + \theta_1, \quad \mathbb{S} = r\sin\alpha + \theta_1. \tag{30}$$

The design parameters can be modified such that $T_k|_{k\neq 0,1}$ depends on six variables. It is observed that four of the design variables, i.e., $\{l_2, x_0, y_0, \theta_1\}$ only exist in the expressions for $T_0$ and $T_1$. As a result, a ten-dimensional search space has been reduced into a six-dimensional space. The four remaining variables can be fitted exactly using the complex equations for fitting $T_0$ and $T_1$. The objective now is to search for optimal $\left\{\frac{l_2}{l_1}, \frac{l_3}{l_1}, \frac{l_4}{l_1}, \phi_0, \mathbb{C}, \mathbb{S}\right\}$.

To find a least square solution to Eq. (27), the minimum for $\mathbb{C}$ and $\mathbb{S}$ is calculated by minimizing the following error function

$$I = \sum_{k\neq 0,1} |C_k re^{i(\alpha+\theta_1+k\phi_0)} - T_k|^2 \tag{31}$$

$$= \sum_{k\neq 0,1} [(A_k \cdot \mathbb{C} - B_k \cdot \mathbb{S} - T_k^x)^2 + (A_k \cdot \mathbb{S} + B_k \cdot \mathbb{C} - T_k^y)^2], \tag{32}$$

where $T_k = T_k^x + iT_k^y$ and $C_k e^{ik\phi_0} = A_k + iB_k$. Setting partial differentials to zero and analytically minimizing the error function leads to

$$\mathbb{C} + i\mathbb{S} = \frac{\sum_{k\neq 0,1} T_k C_k^* e^{-ik\phi_0}}{\sum_{k\neq 0,1} |C_k|^2}. \tag{33}$$

As a result, the least square solution to Eq. (27) can be found by optimization of four design variables namely $\left\{\frac{l_2}{l_1}, \frac{l_3}{l_1}, \frac{l_4}{l_1}, \phi_0\right\}$. The optimization space has thus been reduced to a mere four design variables instead of original ten design variables.

During the discussion, the constraint imposed by the feasibility condition has been ignored. Thus, to generate valid mechanisms, an extra relation needs to be satisfied. Rewriting the feasibility condition in terms of four design variables, we get

$$\left(\frac{l_3}{l_1} - \frac{l_4}{l_1}\right)^2 \leq 1 + \left(\frac{l_2}{l_1}\right)^2 - 2\left(\frac{l_2}{l_1}\right)\cos\phi \leq \left(\frac{l_3}{l_1} + \frac{l_4}{l_1}\right)^2. \tag{34}$$

All $\phi$ in range $[\phi_0,\ \phi_0 + \Phi_{max}]$ must satisfy the inequality for the mechanism to be meaningful. Direct search method has been used as the optimization method in work by Wu et al. [23]. This completes the review of Fourier based path synthesis algorithm.

## 3 Optimum parametrization

Fourier based Path synthesis requires assigning a time parameter to each of the input path points. Using parameterizations other than uniform sampling yields different task curves, which results in a different synthesized mechanism. Thus, an optimum parameterizations scheme is essential to select the best task curve to solve the path problem.

Time parameter is not necessarily a problem which needs to be eliminated. The time dependence of Fourier descriptors can be exploited to give mechanism designers increased flexibility. The time parameter decides when the synthesized mechanism moves over each point. By changing the time distribution, finer control on motion of coupler point can be established.

In practical scenarios, uniform parametrization results in a target curve where the end effector takes equal time to pass through each target point. Thus, the uniform parameter is desired in cases where the relative time between each target point is required to be same. Similarly, for cases where the constant speed of end effector over the target path is required, close to arc length parametrization would be desired. Analytically, it is not possible to get the arc length parametrization before the synthesis process, but a good approximation is the chord length parametrization. Thus, uniform and chord length parametrization are two important parameterizations which have substantial design use-case. A generalized parametrization incorporating both of these cases is thus required.

In interpolation path finding problems, chord length based parameterizations have been used by geometers for a long time. In the case of path synthesis, formulation in Eq. (4) to define open task curve is valid for any parametrization, uniform or nonuniform, over a specified domain $[0, \theta]$. This resultant curve interpolating the input path points can be calculated using a generalized parametrization called centripetal parametrization. It can be represented as

$$t_0 = 0, \tag{35}$$

$$t_k = \frac{\sum_{i=1}^{k} |D_i - D_{i-1}|^{\alpha}}{L}, \tag{36}$$

$$t_n = 1, \tag{37}$$

where $t_k$ represents the parameter for each input path point, $D_i$ represents the cumulative chord length till $i^{th}$ point and $L$ represents the total cumulative chord length till last point. $\alpha$ is the parametrization control variable such that $\alpha \in \mathbb{R}$ and $\alpha \geq 0$. On varying the control variable $\alpha$, multiple parametrization can be generated. It must be noted that uniform and chord length parametrization are special cases when $\alpha = 0$ and $\alpha = 1$, respectively.

From this family of parameterizations, the concern now is to select the best parametrization. Objective it to find specific value of $\alpha$ such that wiggle in the curve is minimized. This can be done by minimizing the total arc length of the curve. Analytically, arc length ($L_a$) is defined as

$$L_a = \int \sqrt{1 + \left(\frac{dz}{dt}\right)^2}\, dt, \tag{38}$$

where $z$ is the task curve and $t$ is the time parameter. Closed form solution for the above integration is not possible.

Fortunately, $L_a$ can also easily be computed numerically by dividing the curve into many intervals and approximate these lengths using a line segment. When the curve is divided into a large number of intervals, a close approximation can be calculated. Thus, finding the best parametrization is a one-dimensional minimization problem with objective function being minimization of arc length. For our implementation, we have used Nelder-Mead method to numerically solve the minimization problem. The Algorithm 1 summarizes this approach.

**Algorithm 1:** Calculation of Optimum Parametrization

**Input:** Initial Parametrization ($\alpha_0$)
**while** *Residue* $> \varepsilon$ **do**
  Move to neighbour $\alpha_i$
  Find new Task curve $z_i = z(\alpha_i)$
  Calculate Arc length $L_{a,i} = L_a(z_i)$
  Calculate Residue=$\|L_{a,i} - L_{a,i-1}\|$
**end**
**Output:** Minimum parametrization ($\alpha$)

## 4 Design-Centric Constraints

Design problems come in many flavors. Usually, large variation in end effector speeds is not desirable. The larger the changes in speed, the larger are the forces induced on links which makes dynamic analysis indispensable in these cases. These large forces can even compromise the rigidity of links making the kinematic analysis useless.

However, uniform speed over the complete motion of end effector is not the ideal solution to this problem. Some degree of speed change is important in mechanisms like quick return mechanism. Thus, the possibility of specifying speed restrictions would greatly benefit the designer.

The ratio of coupler point's maximum speed to minimum speed has been used as control variable denoted as $S_r$. $S_r$ is always greater than one. The user's main interest while designing is to reject mechanisms which do not satisfy $S_r$ for the design problem. For example, the user might want relatively uniform speed mechanisms with $S_r < 2$. This helps the user narrow down on the particular parametrization which has less wiggle and satisfies speed criteria.

Rewriting the formulation for target path Eq. (3) here for reference,

$$z(t) = \sum_{m=-p}^{p} \alpha_m e^{\omega_o m i t} \qquad \forall \quad t \in [0,T], T < 1. \tag{39}$$

and differentiating the above path curve gives the velocity function as

$$v(t) = \sum_{m=-p}^{p} m\beta_m e^{\omega_o m i t}, \tag{40}$$

where $\beta_m = i\omega_o \alpha_m$. To analytically find the maximum and minimum velocities, roots of derivative of Eq. (40) are needed. Then, values of their second derivative at the roots will determine if its a maximum or minimum. Unfortunately, root finding problem for any function is an optimization problem in itself.

To avoid the use of optimization, max and min speeds can be found out by sampling the curve and directly finding the values of velocity using Eq. (40). The magnitude of this complex velocity gives us speed. By taking a large number of samples, a good approximation of $S_r$ can be achieved.

The designer specifies a lower speed ratio bound ($S_{r,min}$) and upper speed ratio bound ($S_{r,max}$). Mechanisms of interest lie exclusively in this region. If no limitations are enforced by the user, then taking $S_{r,min} = 1$ and $S_{r,max} = \infty$ includes all the possible parameterizations.

Penalty functions have been used to convert a constrained optimization problem to an unconstrained one. Literature describing different types of internal and external penalties is rich. The quadratic penalty function is used to include these constraints within the objective function to find the relevant mechanisms. The inequality constraints are

$$S_{r,min} \le S_r(z) \le S_{r,max}, \tag{41}$$

which can be rewritten as following inequalities

$$g_1(z) : S_r(z) - S_{r,min} \ge 0, \tag{42}$$

$$g_2(z) : S_{r,max} - S_r(z) \ge 0. \tag{43}$$

The new objective function to find optimum parametrization by minimizing both the arc length and velocity penalty functions becomes

$$f(z) = L_a(z) + P(max(0, -g_1(z)) + max(0, -g_2(z)))^2, \tag{44}$$

where $z$ is task curve, $L_a$ is arc length, $g_1, g_2$ are constraints and $P$ is the penalty. Tweaking $P$ can lead to good results numerically.

Thus, a method to find a target Fourier curve which has minimum wiggle and is constrained by min- max speed has been outlined above. Using this methodology, the influence of time parametrization on the path is effectively minimized. If the design requirement is of uniform time or speed parametrization, $\alpha$ can directly be set to 0 or 1. If multiple solutions are required for a problem, a variety of task curve parameterizations can be used to generate multiple solutions.

The complete Fourier based path synthesis algorithm using optimum parametrization has been summarized in Algorithm 2. We have used simulated annealing as the optimization technique for the minimization problem.

**Algorithm 2:** Solving the Path Synthesis problem

**Input:** Set of Path points
1. Calculate Task curve Fourier descriptors using Optimum parametrization.
2. Fit the Coupler curve to Optimum Task curve and synthesize a four-bar mechanism.

**Output:** Four-bar mechanism parameters

## 5 Examples

In this section, a few examples are presented to demonstrate the proposed algorithm. First example compares a variety of parameterizations with optimal parametrization. Second example seeks to test our algorithm to generate an existing four-bar mechanism by inputting its coupler points. Third example tests our algorithm against an unknown set of path points. Fourth example tests the design-centric velocity constraints on task curve. The last example displays multiple solutions found for same set of path points using different parameterizations. Green curves have been used to represent task curves while blue curves denote the coupler point paths. The red curves represent coupler path if the mechanism is assembled in alternate configuration.

### 5.1 Example 1: Task Curve Comparison

A sample case, for data listed in Table 1, has been shown in Figs. 2, 3, 4 where least square fitted trigonometric curve is generated for five sample input points using different parametrization techniques. The wiggle in the first two cases is very apparent in the first two curve. The third curve is relatively better than the other two. This begs the question, for which value of $\alpha$ does the best parametrization exists.

**TABLE 1**: Example 1: Input Path Point Data to analyze effect on Task path under different parameterizations

| X | Y |
|---|---|
| −6.065 | 1.541 |
| −4.298 | 2.218 |
| −2.982 | 2.519 |
| −0.589 | 2.444 |
| 4.436 | −1.779 |

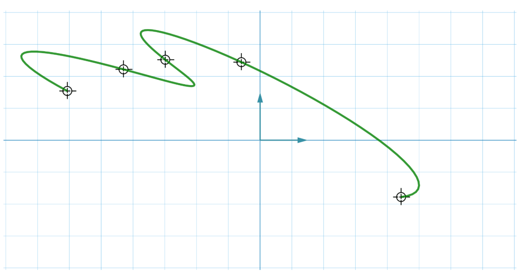

**FIGURE 2**: Example 1: Task curve calculated using Uniform Parametrization ($\alpha = 0$)

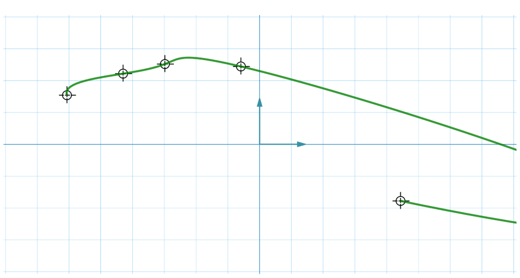

**FIGURE 3**: Example 1: Task curve calculated using Chordal Parametrization ($\alpha = 1$)

The proposed optimal parametrization algorithm calculates that the minimum arc length occurs at $\alpha = .4875$ for the sample test-case. Fig. 5 displays the Task curve generated using optimal

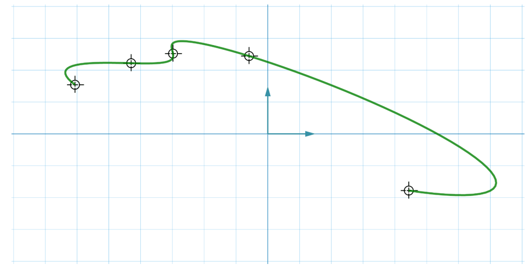

**FIGURE 4**: Example 1: Task curve calculated using Centripetal Parametrization ($\alpha = .5$)

parametrization. Fourier descriptors for each curve are described in Table 2.

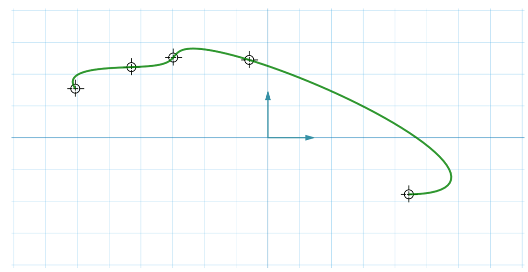

**FIGURE 5**: Example 1: Task curve calculated using Optimum Parametrization ($\alpha = .4875$)

**TABLE 2**: Example 1: Task path Descriptor Data for Parameterizations in Fig. 2, 3, 4, 5

| | Task path $\alpha = 0$ | | Task path $\alpha = 1$ | |
|---|---|---|---|---|
| Descriptor | Complex Value | Magnitude | Complex Value | Magnitude |
| p=−2 | $-1.953-0.089i$ | 1.9552 | $-0.424+1.532i$ | 1.5893 |
| p=−1 | $-1.355-2.423i$ | 2.7763 | $-4.508-2.595i$ | 5.2015 |
| p=0 | $-1.910+1.404i$ | 2.3700 | $1.727+0.468i$ | 1.7890 |
| p=1 | $0.155+1.477i$ | 1.4847 | $-1.892+3.221i$ | 3.7360 |
| p=2 | $-1.002+1.174i$ | 1.5433 | $-0.967-1.085i$ | 1.4533 |
| | Task path $\alpha = .5$ | | Task path $\alpha = .4875$ | |
| Descriptor | Complex Value | Magnitude | Complex Value | Magnitude |
| p=−2 | $-1.159+0.934i$ | 1.4888 | $-0.719+0.979i$ | 1.2147 |
| p=−1 | $-2.539-2.550i$ | 3.5983 | $-2.759-1.960i$ | 3.3841 |
| p=0 | $-0.729+1.054i$ | 1.2816 | $-1.033+1.025i$ | 1.4555 |
| p=1 | $-0.432+2.173i$ | 2.2154 | $-0.679+1.752i$ | 1.8792 |
| p=2 | $-1.205-0.069i$ | 1.2075 | $-0.875-0.255i$ | 0.9110 |

## 5.2 Example 2: Synthesizing Existing Mechanisms

To test the ability of Path Synthesis to create existing mechanisms, a sample mechanism is taken, points from its coupler path are sampled and then a mechanism is synthesized which goes through the sampled points. Ideally, we should get the exact same mechanism. However, a similar mechanism is also acceptable since the premise is of approximate synthesis.

A sample mechanism as visualized in Fig. 6 has been used to generate coupler path positions. The mechanism has been defined using the position of its fixed pivots, moving pivots and coupler coordinates as shown in Table 3. Coupler curve of this mechanism is sampled and used as input for Path Synthesis algorithm. The least square curves are approximated with seven Fourier Descriptors for this test cases.

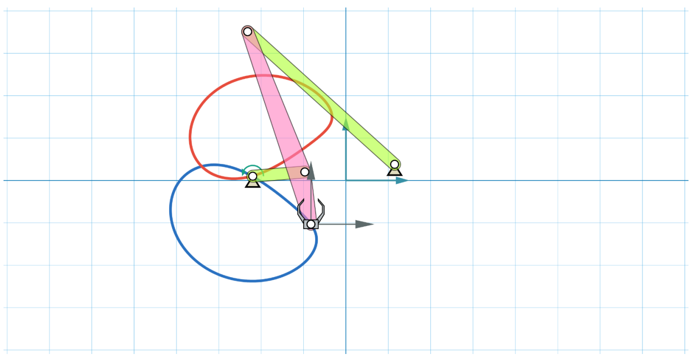

**FIGURE 6**: Example 2: Path data Generator mechanism used to analyze effect on Path Synthesis under different parameterizations

**TABLE 3**: Example 2: Path data Generator Mechanism design parameters as shown in Fig. 6

| Point | X | Y |
|---|---|---|
| Input link fixed pivot | −2.20 | 0.10 |
| Input link moving pivot | −0.97 | 0.20 |
| Output link fixed pivot | 1.15 | 0.38 |
| Output link moving pivot | −2.32 | 3.51 |
| Coupler Point | −0.825 | −1.033 |

We now compare the use of optimum and uniform parameterizations for the sampled data. The randomly sampled coupler curve data used for testing contains ten path points and is given in Table 4. Fig. 7 represents the uniform parametrization case while Fig. 8 represents the optimum parametrization case. Table 5 and Table 7 contains the Fourier descriptor and Synthesized mechanism data for uniform parametrization while Table 6 and Table 8 shows same for optimum parametrization which occurs at $\alpha = .9188$. It is observed that optimum parametrization yields better result than uniform parametrization.

**TABLE 4**: Example 2: Input non-uniformly sampled point data to analyze effect of Path Synthesis under different parameterizations

| X | Y |
|---|---|
| −0.825 | −1.033 |
| −1.249 | −0.600 |
| −2.918 | 0.360 |
| −3.287 | 0.363 |
| −3.521 | 0.302 |
| −4.038 | −0.178 |
| −4.151 | −0.635 |
| −3.541 | −1.905 |
| −1.864 | −2.352 |
| −0.692 | −1.442 |

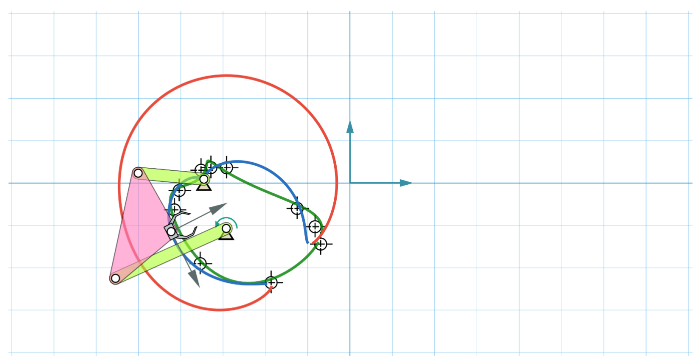

**FIGURE 7**: Example 2: Synthesized mechanism for non-uniformly sampled input using uniform parametrization

The uniform parametrization result is fundamentally different from the initial mechanism which was a crank-rocker mechanism. This can be attributed to the fact that task curve calculated with uniform parametrization was poor and could not be fitted with a four bar coupler path. The fit for task curve calculated with optimal parameterization is extremely good and the coupler path overlaps most of the task curve.

It must be noted that the mechanisms found using optimization techniques are guaranteed local optimum. However, it is uncertain if these are actually the global minimum in search space.

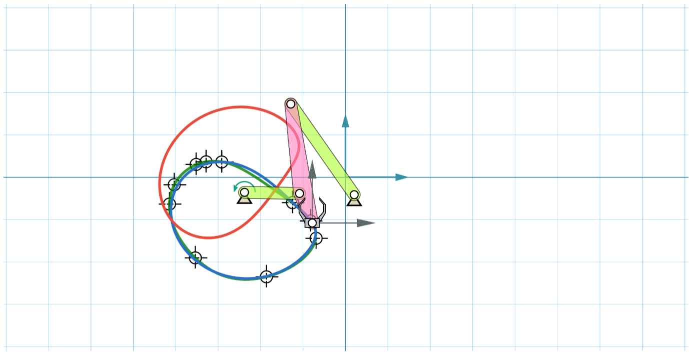

**FIGURE 8**: Example 2: Synthesized mechanism for non-uniformly sampled input using optimum parametrization

**TABLE 5**: Example 2: Task path and Coupler path Descriptor Data for Fig. 7

| | Task path | | Coupler path | |
|---|---|---|---|---|
| Descriptor | Complex Value | Magnitude | Complex Value | Magnitude |
| p=−3 | $0.050+0.124i$ | 0.1336 | $0.007-0.015i$ | 0.0165 |
| p=−2 | $0.141-0.044i$ | 0.1478 | $0.010-0.023i$ | 0.0250 |
| p=−1 | $0.243-0.219i$ | 0.3267 | $0.124-0.101i$ | 0.1597 |
| p=0 | $-2.774-0.664i$ | 2.8520 | $-2.774-0.664i$ | 2.8520 |
| p=1 | $1.279-0.529i$ | 1.3840 | $1.279-0.529i$ | 1.3840 |
| p=2 | $0.407+0.109i$ | 0.4209 | $0.449+0.116i$ | 0.4636 |
| p=3 | $-0.011+0.044i$ | 0.0450 | $-0.091+0.024i$ | 0.0939 |

**TABLE 6**: Example 2: Task path and Coupler path Descriptor Data for Fig. 8

| | Task path | | Coupler path | |
|---|---|---|---|---|
| Descriptor | Complex Value | Magnitude | Complex Value | Magnitude |
| p=−3 | $0.024-0.021i$ | 0.0324 | $0.027-0.024i$ | 0.0360 |
| p=−2 | $0.074-0.035i$ | 0.0821 | $0.067-0.050i$ | 0.0836 |
| p=−1 | $0.138-0.198i$ | 0.2410 | $0.144-0.192i$ | 0.2396 |
| p=0 | $-2.502-1.019i$ | 2.7016 | $-2.502-1.019i$ | 2.7016 |
| p=1 | $1.489+0.140i$ | 1.4954 | $1.489+0.140i$ | 1.4954 |
| p=2 | $-0.034+0.052i$ | 0.0625 | $-0.018+0.061i$ | 0.0632 |
| p=3 | $-0.001+0.051i$ | 0.0507 | $-0.010+0.009i$ | 0.0136 |

**TABLE 7**: Example 2: Synthesized mechanism parameters Data for Fig. 7

| $l_1$ | $l_2$ | $l_3$ | $l_4$ | $x_0$ | $y_0$ |
|---|---|---|---|---|---|
| 1.277 | 2.871 | 2.540 | 1.560 | −2.925 | −1.073 |

| $\theta_1$ | $r$ | $\alpha$ | $\phi_0$ |
|---|---|---|---|
| 1.998 | 1.716 | −0.660 | 3.620 |

**TABLE 8**: Example 2: Synthesized mechanism parameters Data for Fig. 8

| $l_1$ | $l_2$ | $l_3$ | $l_4$ | $x_0$ | $y_0$ |
|---|---|---|---|---|---|
| 2.588 | 1.298 | 2.122 | 2.612 | −2.381 | −0.358 |

| $\theta_1$ | $r$ | $\alpha$ | $\phi_0$ |
|---|---|---|---|
| −0.022 | 0.759 | −2.832 | 0.001 |

Simulated Annealing only guarantees global minimum asymptotically over a long time. As mentioned earlier, faster solutions have been preferred in our implementation. Longer runtime might yield better solutions.

### 5.3 Example 3: Multiple solutions

In this example, we synthesize multiple four-bar mechanisms for same set of input points. The input data used for this case is a set of eight path points as given in Table 9. A variety of mechanisms can be synthesized easily by running the algorithm for different values of parametrization control variable $\alpha$. This results in a slightly different fitted task curve which changes the end result. Fig. 9, Fig. 10, and Fig. 11 represents mechanisms synthesized at $\alpha = .25, .5, .75$, respectively. Table 10, Table 11, and Table 12 displays the Fourier descriptors for each case while Table 13, Table 14 and Table 15 displays the synthesized mechanism parameters. Thus, multiple solutions can be generated using different parameterizations for task path.

**TABLE 9**: Example 3: Input path point data to generate multiple solutions for Path Synthesis Problem

| X | Y |
|---|---|
| −0.802 | 1.278 |
| −1.341 | 1.090 |
| −2.444 | 0.401 |
| −3.672 | −0.714 |
| −2.757 | −1.078 |
| −0.501 | −1.153 |
| 0.564 | −0.539 |
| 0.551 | 0.627 |

Note the diverse variety of coupler path geometry i.e. open, closed or self-intersecting profiles in the generated mechanisms. Also, it can be observed that minor change in the task curve can result in extremely different solutions. This approach provides the user immense flexibility to generate multiple mechanisms without changing any of the input path constraints.

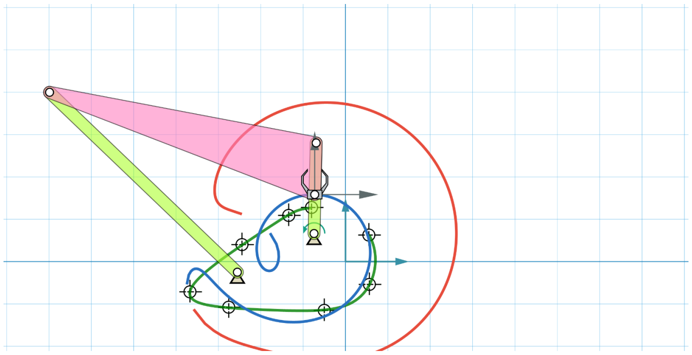

**FIGURE 9**: Example 3: Synthesized mechanism for input using parametrization control parameter $\alpha = .25$

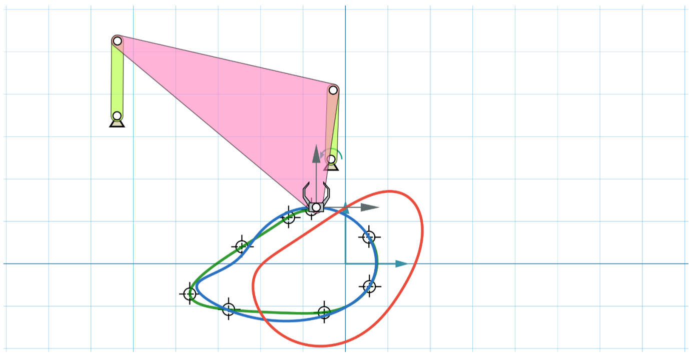

**FIGURE 10**: Example 3: Synthesized mechanism for input using parametrization control parameter $\alpha = .5$

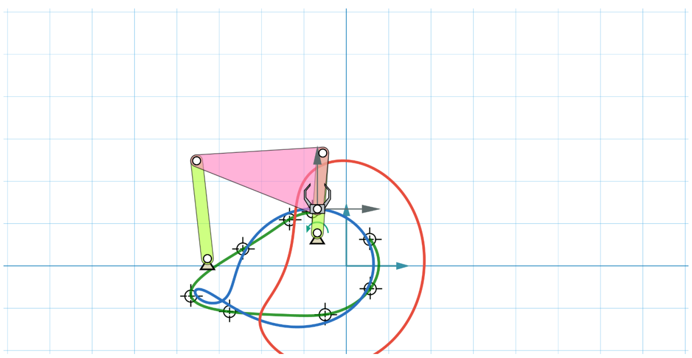

**FIGURE 11**: Example 3: Synthesized mechanism for input using parametrization control parameter $\alpha = .75$

**TABLE 10**: Example 3: Task path and Coupler path Descriptor Data for Fig. 9

| | Task path | | Coupler path | |
|---|---|---|---|---|
| Descriptor | Complex Value | Magnitude | Complex Value | Magnitude |
| p=−3 | $-0.054-0.068i$ | 0.0872 | $-0.156-0.092i$ | 0.1817 |
| p=−2 | $-0.064+0.244i$ | 0.2525 | $-0.017+0.239i$ | 0.2391 |
| p=−1 | $0.320-0.261i$ | 0.4125 | $0.322-0.133i$ | 0.3487 |
| p=0 | $-1.259+0.004i$ | 1.2591 | $-1.259+0.004i$ | 1.2591 |
| p=1 | $0.450+1.551i$ | 1.6149 | $0.450+1.551i$ | 1.6149 |
| p=2 | $-0.109-0.182i$ | 0.2120 | $-0.132-0.059i$ | 0.1450 |
| p=3 | $-0.086-0.023i$ | 0.0885 | $-0.077+0.060i$ | 0.0976 |

**TABLE 11**: Example 3: Task path and Coupler path Descriptor Data for Fig. 10

| | Task path | | Coupler path | |
|---|---|---|---|---|
| Descriptor | Complex Value | Magnitude | Complex Value | Magnitude |
| p=−3 | $-0.066-0.036i$ | 0.0752 | $-0.064-0.008i$ | 0.0642 |
| p=−2 | $-0.040+0.212i$ | 0.2156 | $-0.028+0.159i$ | 0.1611 |
| p=−1 | $0.311-0.284i$ | 0.4211 | $0.333-0.259i$ | 0.4218 |
| p=0 | $-1.305-0.066i$ | 1.3072 | $-1.305-0.066i$ | 1.3072 |
| p=1 | $0.491+1.543i$ | 1.6193 | $0.491+1.543i$ | 1.6193 |
| p=2 | $-0.082-0.079i$ | 0.1138 | $-0.152-0.043i$ | 0.1578 |
| p=3 | $-0.113-0.024i$ | 0.1151 | $-0.022+0.024i$ | 0.0328 |

**TABLE 12**: Example 3: Task path and Coupler path Descriptor Data for Fig. 11

| | Task path | | Coupler path | |
|---|---|---|---|---|
| Descriptor | Complex Value | Magnitude | Complex Value | Magnitude |
| p=−3 | $-0.078-0.014i$ | 0.0790 | $-0.102-0.028i$ | 0.1056 |
| p=−2 | $-0.001+0.180i$ | 0.1795 | $0.039+0.193i$ | 0.1971 |
| p=−1 | $0.293-0.305i$ | 0.4234 | $0.291-0.273i$ | 0.3991 |
| p=0 | $-1.339-0.124i$ | 1.3450 | $-1.339-0.124i$ | 1.3450 |
| p=1 | $0.493+1.538i$ | 1.6155 | $0.493+1.538i$ | 1.6155 |
| p=2 | $-0.040+0.003i$ | 0.0405 | $-0.091+0.037i$ | 0.0987 |
| p=3 | $-0.137-0.016i$ | 0.1377 | $-0.035+0.004i$ | 0.0351 |

### 5.4 Example 4: Design-Centric Constraints

This example demonstrates the effect of design-centric constraints on synthesized four-bar mechanism. The input data used for this case is a set of six path points as given in Table 16. The design-centric constraint fixes the speed ratios to 5. Fig. 12 represents the optimal parametrization case without the design-centric constraint while Fig. 13 represents the optimum parametrization case with design-centric constraint applied. The parametrization control variable is calculated to be $\alpha = .1103$ for case without constraint and $\alpha = .6594$ for case with constraint. Table 18 and Table 20 contains the Fourier descriptor and Synthesized mech-

**TABLE 13**: Example 3: Synthesized mechanism parameters Data for Fig. 9

| $l_1$ | $l_2$ | $l_3$ | $l_4$ | $x_0$ | $y_0$ |
|---|---|---|---|---|---|
| 2.027 | 2.140 | 6.406 | 6.141 | −0.742 | 0.662 |

| $\theta_1$ | $r$ | $\alpha$ | $\phi_0$ |
|---|---|---|---|
| −2.674 | 1.220 | 1.730 | 4.222 |

**TABLE 14**: Example 3: Synthesized mechanism parameters Data for Fig. 10

| $l_1$ | $l_2$ | $l_3$ | $l_4$ | $x_0$ | $y_0$ |
|---|---|---|---|---|---|
| 5.149 | 1.629 | 5.217 | 1.764 | −0.341 | 2.466 |

| $\theta_1$ | $r$ | $\alpha$ | $\phi_0$ |
|---|---|---|---|
| 2.941 | 2.792 | −4.631 | 4.881 |

**TABLE 15**: Example 3: Synthesized mechanism parameters Data for Fig. 11

| $l_1$ | $l_2$ | $l_3$ | $l_4$ | $x_0$ | $y_0$ |
|---|---|---|---|---|---|
| 2.663 | 1.890 | 2.984 | 2.326 | −0.686 | 0.781 |

| $\theta_1$ | $r$ | $\alpha$ | $\phi_0$ |
|---|---|---|---|
| −2.911 | 1.327 | 1.414 | 4.413 |

anism data for optimal parametrization case without the design-centric constraint. Table 17 and Table 19 shows descriptors for optimum parametrization with design constraint. It is observed that both of them yield different mechanism. The velocity plots in Fig 14 show that there is reduced variation in second case. Thus, the design-centric constraints can help synthesize a better four-bar mechanism with desirable speed variation.

**TABLE 16**: Example 4: Input path point data to analyze effect of Path Synthesis under design-centric constraints

| X | Y |
|---|---|
| −5.088 | −0.576 |
| −3.897 | −0.338 |
| −3.158 | 0.840 |
| −2.581 | 1.391 |
| 0.990 | −1.028 |
| 0.025 | −2.995 |

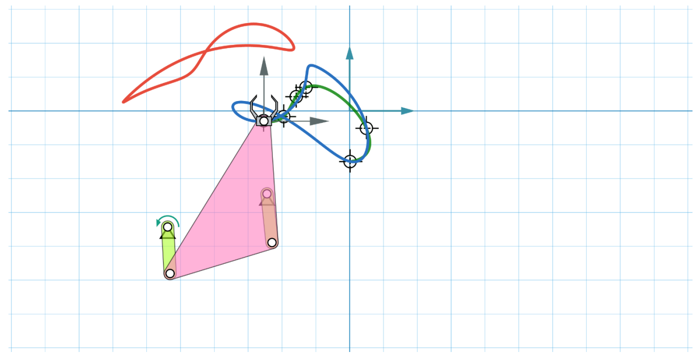

**FIGURE 12**: Example 4: Synthesized mechanism for input using optimal parametrization without design-centric constraint

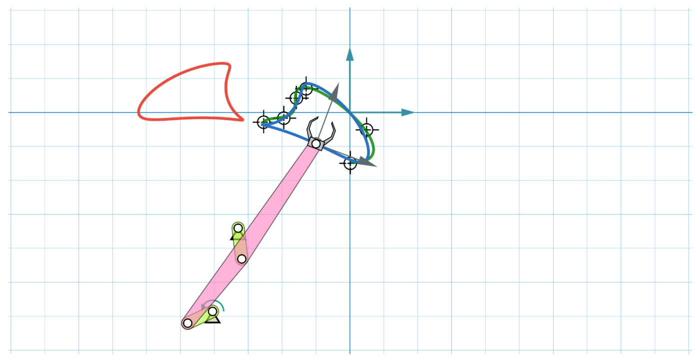

**FIGURE 13**: Example 4: Synthesized mechanism for input using optimal parametrization with design-centric constraint

**TABLE 17**: Example 4: Task path and Coupler path Descriptor Data for Fig. 13

| | Task path | | Coupler path | |
|---|---|---|---|---|
| Descriptor | Complex Value | Magnitude | Complex Value | Magnitude |
| p=−2 | $1.024-1.336i$ | 1.6839 | $1.024-1.336i$ | 1.6839 |
| p=−1 | $-0.696+3.302i$ | 3.3741 | $-0.696+3.302i$ | 3.3741 |
| p=0 | $-4.988+0.163i$ | 4.9906 | $-4.988+0.163i$ | 4.9906 |
| p=1 | $-1.416-2.093i$ | 2.5266 | $-1.416-2.093i$ | 2.5266 |
| p=2 | $0.981-0.616i$ | 1.1588 | $0.981-0.616i$ | 1.1588 |

## 6 Conclusion

In this paper, we have presented a scheme defining family of non-uniform parametrization scheme for Fourier descriptor based path synthesis of a four-bar mechanism. Original contributions include establishing optimality criteria based on minimization of arc length to find the optimal parametrization. Additional design-centric constraints have been proposed to help user establish some control over the coupler speed. The flexibility

**TABLE 18**: Example 4: Task path and Coupler path Descriptor Data for Fig. 12

| | Task path | | Coupler path | |
|---|---|---|---|---|
| Descriptor | Complex Value | Magnitude | Complex Value | Magnitude |
| p=−2 | $-0.211+0.804i$ | 0.8313 | $-0.157+0.716i$ | 0.7331 |
| p=−1 | $-1.849-1.210i$ | 2.2096 | $-1.819-1.227i$ | 2.1943 |
| p=0 | $-2.307-0.607i$ | 2.3854 | $-2.307-0.607i$ | 2.3854 |
| p=1 | $-0.187+0.501i$ | 0.5350 | $-0.187+0.501i$ | 0.5350 |
| p=2 | $-0.567-0.120i$ | 0.5795 | $-0.717-0.078i$ | 0.7214 |

**TABLE 19**: Example 4: Synthesized mechanism parameters Data for Fig. 13

| $l_1$ | $l_2$ | $l_3$ | $l_4$ | $x_0$ | $y_0$ |
|---|---|---|---|---|---|
| 6.189 | 2.754 | 6.297 | 2.894 | −10.761 | −6.860 |

| $\theta_1$ | $r$ | $\alpha$ | $\phi_0$ |
|---|---|---|---|
| 0.322 | 10.577 | 0.723 | 4.443 |

**TABLE 20**: Example 4: Synthesized mechanism parameters Data for Fig. 12

| $l_1$ | $l_2$ | $l_3$ | $l_4$ | $x_0$ | $y_0$ |
|---|---|---|---|---|---|
| 5.127 | 1.622 | 4.947 | 1.826 | −8.102 | −11.715 |

| $\theta_1$ | $r$ | $\alpha$ | $\phi_0$ |
|---|---|---|---|
| 1.272 | 12.997 | 0.079 | 3.176 |

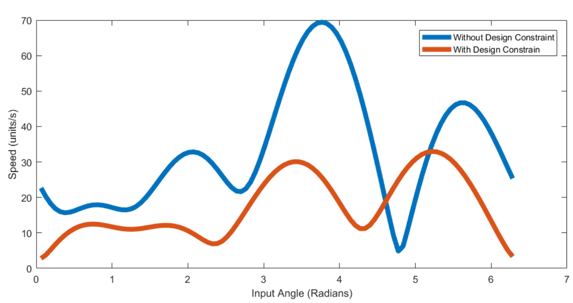


**FIGURE 14**: Example 4: Comparison of speed for the two mechanisms generated

provided to the user helping him generate more than one mechanisms based on different parametrization is also novel. Many examples have been presented to display the immense usefulness of the model over previous Fourier based path synthesis algorithms. By incorporating parameterizations which were neglected previously, the proposed framework proves to be a generalized approach to path synthesis for four-bar mechanisms.


## ACKNOWLEDGMENT

This work has been financially supported by National Science Foundation under a research grant to Stony Brook University (PI: A. Purwar and Co-PI: Q.J. Ge, grant CMMI-1563413). All findings and results presented in this paper are those of the authors and do not represent those of the funding agencies.


## REFERENCES


[1] Freudenstein, F., 1954. "An analytical approach to the design of four-link mechanisms". *Trans. ASME,* ***76***(3), pp. 483–492.

[2] Hartenberg, R. S., and Denavit, J., 1964. *Kinematic Synthesis of Linkages*. McGraw-Hill, New York.

[3] Blechschmidt, J. L., and Uicker, J. J., 1986. "Linkage synthesis using algebraic-curves". *Journal of Mechanisms Transmissions and Automation in Design-Transactions of the Asme,* ***108***(4), pp. 543–548.

[4] Suh, C. H., and Radcliffe, C. W., 1978. *Kinematics and Mechanism Design*. John Wiley and Sons, New York.

[5] Erdman, A. G., and Sandor, G. N., 1991. *Advanced Mechanism Design: Analysis and Synthesis*, 2nd ed., Vol. 2. Prentice-Hall, Englewood Cliffs, NJ.

[6] Nolle, H., and Hunt, K. H., 1971. "Optimum synthesis of planar linkages to generate coupler curves". *Journal of Mechanisms,* ***6***(3), p. 267.

[7] Fox, R. L., and Gupta, K. C., 1973. "Optimization technology as applied to mechanism design". *Journal of Engineering for Industry-Transactions of the Asme,* ***95***(2), pp. 657–662.

[8] Bagci, C., and Lee, I.-P. J., 1975. "Optimum synthesis of plane mechanisms for the generation of paths and rigid-body positions via the linear superposition technique". *Journal of Engineering for Industry,* ***97***(1), pp. 340–346.

[9] Angeles, J., Alivizatos, A., and Akhras, R., 1988. "An unconstrained nonlinear least-square method of optimization of rrrr planar path generators". *Mechanism and Machine Theory,* ***23***(5), pp. 343–353.

[10] Sancibrian, R., Viadero, F., Garcia, P., and Fernandez, A., 2004. "Gradient-based optimization of path synthesis problems in planar mechanisms". *Mechanism and Machine Theory,* ***39***(8), pp. 839–856.

[11] Smaili, A. A., Diab, N. A., and Atallah, N. A., 2005. "Optimum synthesis of mechanisms using tabu-gradient search algorithm". *Journal of Mechanical Design,* ***127***(5), pp. 917–923.

[12] Smaili, A., and Diab, N., 2007. "Optimum synthesis of hybrid-task mechanisms using ant-gradient search

method". *Mechanism and Machine Theory,* ***42***(1), pp. 115–130.

[13] Ullah, I., and Kota, S., 1997. "Optimal synthesis of mechanisms for path generation using fourier descriptors and global search methods". *Journal of Mechanical Design,* ***119***(4), pp. 504–510.

[14] Martnez-Alfaro, H., 2007. *Four-bar mechanism synthesis for n desired path points using simulated annealing*. Springer, pp. 23–37.

[15] Zhou, H., and Cheung, E. H., 2001. "Optimal synthesis of crankrocker linkages for path generation using the orientation structural error of the fixed link". *Mechanism and Machine Theory,* ***36***(8), pp. 973–982.

[16] Marn, F. T. S., and Gonzlez, A. P., 2003. "Global optimization in path synthesis based on design space reduction". *Mechanism and machine theory,* ***38***(6), pp. 579–594.

[17] Smaili, A., and Diab, N., 2007. "A new approach to shape optimization for closed path synthesis of planar mechanisms". *Journal of Mechanical Design,* ***129***(9), pp. 941–948.

[18] Watanabe, K., 1992. "Application of natural equations to the synthesis of curve generating mechanisms". *Mechanism and Machine Theory,* ***27***(3), pp. 261–273.

[19] Hoeltzel, D. A., and Chieng, W. H., 1990. "Pattern-matching synthesis as an automated approach to mechanism design". *Journal of Mechanical Design,* ***112***(2), pp. 190–199.

[20] Vasiliu, A., and Yannou, B., 2001. "Dimensional synthesis of planar mechanisms using neural networks: application to path generator linkages". *Mechanism and Machine Theory,* ***36***(2), pp. 299–310.

[21] Galan-Marin, G., Alonso, F. J., and Del Castillo, J. M., 2009. "Shape optimization for path synthesis of crank-rocker mechanisms using a wavelet-based neural network". *Mechanism and Machine Theory,* ***44***(6), pp. 1132–1143.

[22] Efrat, A., Fan, Q. F., and Venkatasubramanian, S., 2007. "Curve matching, time warping, and light fields: New algorithms for computing similarity between curves". *Journal of Mathematical Imaging and Vision,* ***27***(3), pp. 203–216.

[23] Wu, J., Ge, Q. J., Gao, F., and Guo, W. Z., 2010. "On the extension of a fourier descriptor based method for four-bar linkage synthesis for generation of open and closed paths". In 2010 ASME Mechanisms and Robotics Conference. DETC2010–29028.

[24] Wu, J., Ge, Q. J., and Gao, F., 2009. "An efficient method for synthesizing crank-rocker mechanisms for generating low harmonic curves". In ASME 2009 International Design Engineering Technical Conferences and Computers and Information in Engineering Conference, Vol. 2009. DETC2009-87140.

[25] Mcgarva, J., and Mullineux, G., 1993. "Harmonic representation of closed curves". *Applied Mathematical Modelling,* ***17***(4), pp. 213–218.

[26] Li, X. Y., and Chen, P., 2017. "A parametrization-invariant fourier approach to planar linkage synthesis for path generation". *Mathematical Problems in Engineering,* ***2017***.

 